Heterogeneous Interactions of NO2 with Aqueous Surfaces

ARTICLE *in* THE JOURNAL OF PHYSICAL CHEMISTRY A · MARCH 2000

Impact Factor: 2.69 · DOI: 10.1021/jp992929f

Heterogeneous Interactions of NO_2 with Aqueous Surfaces

J. L. Cheung, Y. Q. Li, J. Boniface, Q. Shi, and P. Davidovits*

Chemistry Department, Merkert Chemistry Center, Boston College, Chestnut Hill, Massachusetts 02467

D. R. Worsnop, J. T. Jayne, and C. E. Kolb

Center for Aerosol and Cloud Chemistry, Aerodyne Research Inc., 45 Manning Road, Billerica, Massachusetts 01821

Received: August 19, 1999; In Final Form: January 11, 2000

Uptake of gas-phase NO_2 by water was studied in both the droplet train and bubble train flow reactors. Aqueous surface reaction of $NO_2(g)$, reported previously in the literature, is not substantiated by these studies. The uptake of $NO_2(g)$ is a function of Henry's law coefficient (H_{NO_2}) and the second-order $NO_2(aq)-NO_2(aq)$ hydrolysis reaction rate coefficient (k_2), in the form $H_{NO_2}(k_2)^{1/2}$. The $NO_2(aq)-NO_2(aq)$ hydrolysis rate coefficient is defined by: $-d[NO_2(aq)]/dt = 2k_2[NO_2(aq)]^2$. The coupled nature of the uptake makes it difficult to obtain reliable separate values for the two parameters H and k_2. Literature values for these parameters vary by as much as a factor of 5. With the bubble train apparatus it was possible to separate clearly the effects of solubility and reaction on NO_2 gas uptake. From these measurements and analysis of literature values, recommended values of these parameters at 293 K are $H_{NO_2} = (1.4 \pm 0.2) \times 10^{-2}$ M atm^{-1} and $k_2 = (3.0 \pm 0.9) \times 10^7$ M^{-1} s^{-1}. At 276 K, our best estimates are $H_{NO_2} = 2.3\ (+0.3-0.9) \times 10^{-2}$ M atm^{-1} and $k_2 = (2.2 \pm 0.6) \times 10^7$ M^{-1} s^{-1}.

Introduction

Nitrogen dioxide is involved in several important atmospheric processes, among them the catalytic production and destruction of stratospheric ozone, the production of tropospheric ozone, and the production of nitric and nitrous acids (HNO_3 and HNO_2). In turn, nitrous acid is photolyzed to form the OH radical, which is the most important oxidizing species in the troposphere. In recent years a considerable amount of work has been directed toward understanding the atmospheric chemistry of $NO_2(g)$ (see reviews by Lammel and Cape,[1] and Schwartz and White[2]). Still, important aspects of its chemistry remain unexplained. For example, field measurements in both rural and urban areas show that the ambient HNO_2/NO_x ratio is much higher than expected from known sources and sinks for HNO_2.[1] On the other hand, measured HNO_3/NO_x ratios in the remote lower free troposphere are lower by about a factor of 5 to 10 than predicted by gas-phase steady-state models.[3] In both cases heterogeneous $NO_2(g)$ interactions have been suggested as possible explanations for the discrepancy.[4−6] Several previous studies have indicated that surface-specific NO_2/water interactions may deviate from expected second-order reaction kinetics of NO_2 with bulk water.[7] A clear understanding of heterogeneous $NO_2(g)$ interactions is central to clarifying these and other issues involving the fate of NO_2 in the atmosphere. In this work, we address three issues related to the interactions of gas-phase NO_2 with pure liquid water: (1) a reported $NO_2(g)$ surface reaction at the aqueous interface, (2) uncertainties in the values of Henry's law coefficient (H_{NO_2}), and (3) uncertainties in the second-order rate coefficient (k_2) for the $NO_2(aq)-NO_2(aq)$ hydrolysis reaction.

Recently, Ponche et al.[8] and Mertes and Wahner[9] performed $NO_2(g)$ uptake experiments using liquid droplet train and liquid jet techniques, respectively. Both studies reported an $NO_2(g)$ uptake rate a factor of 1000 higher than predicted by bulk-phase solubility and reaction. Mertes and Wahner[9] observed that the uptake rate increases with increasing $NO_2(g)$ density and proposed that the high uptake is due to the formation of an NO_2 surface species which then reacts on the surface to form nitric and nitrous acids. To verify their observations, we reexamined the $NO_2(g)$ uptake using both droplet train and bubble train flow reactors.

The Henry's law coefficient, H_{NO_2} and the rate of the second-order hydrolysis reaction, k_2, are two of the key parameters required to characterize heterogeneous processes involving $NO_2(g)$. However, even after several studies,[10−12] uncertainty still exists in the values for these two parameters. Literature values range from 7×10^{-3} to 2×10^{-2} M atm^{-1} for H_{NO_2}, and from 10^7 to 10^8 M^{-1} s^{-1} for k_2 at 25 °C. These uncertainties are due mainly to the complexity of $NO_2(g)$ aqueous interactions.

Previous measurements fall into two categories: NO_2 gas uptake from vertically rising bubbles[10,11,13] and direct kinetic studies of $NO_2(aq)$ or $N_2O_4(aq)$ hydrolysis.[14−16] Each type of study has its complications. Inaccuracies in the $NO_2(aq)$ concentration measurement can affect the measured rate coefficient in the direct liquid-phase kinetic studies. For the $NO_2(g)$ uptake studies, the uptake rate depends both on $NO_2(g)$ solubility and the rate of the solvated $NO_2(aq)-NO_2(aq)$ hydrolysis reaction. These processes are coupled and in most previous gas uptake studies only the product $H_{NO_2}k_2^{1/2}$ was measured; individual H_{NO_2} and k_2 values were estimated by extrapolation. Further, NO_2 forms a dimer, N_2O_4, in both the gas and aqueous phases. Since the dimer is highly soluble, at high $NO_2(g)$ concentrations a significant fraction of the species exists as $N_2O_4(aq)$, affecting solubility measurements at high $NO_2(g)$ concentrations. In addition, measurements involving gas bubble/liquid interactions are complicated by the fact that the

* Corresponding author.

10.1021/jp992929f CCC: $19.00
Published on Web 02/29/2000

liquid forming the walls of the moving bubble is not stationary. The motion of the bubble induces complex flows at the gas−liquid interface which mix the solvated NO_2(aq) deeper into the bulk liquid, thereby reducing the Henry's law solubility constraints. Quantitative interpretation of the uptake data requires modeling of the convective liquid transport at the gas−liquid interface with parameters obtained by careful calibration of the instrument.

To obtain a new set of H_{NO_2} and k_2 values, we performed a series of NO_2(g) uptake studies using a recently developed horizontal bubble train flow reactor. The key differences between previous measurements and the present one is the careful and detailed calibration of the device and the clear control of the gas−liquid interaction time which is determined to a fraction of a second. By ensuring that the bulk liquid does not reach saturation, and by performing uptake measurements as a function of NO_2(g) density, the effect of both solubility and aqueous phase NO_2(aq)−NO_2(aq) reaction can be separated.

Experimental Methods

Both the droplet train and the horizontal bubble train flow reactors have been described elsewhere.[17,18] Here we will present only a brief description of their operation.

Droplet Train Apparatus. In the droplet train flow reactor a fast-moving (1500−3000 cm s^{-1}), monodisperse, and spatially collimated train of aqueous droplets is produced by passing a pressurized liquid through an orifice vibrated by a piezoelectric crystal. The size of the droplets is controlled by the size of the orifice and the frequency of orifice vibration. In the present experiment the droplet diameter is in the range 150−300 μm, depending on experimental conditions. The droplet train passes through a 30 cm longitudinal low-pressure (6−20 Torr) flow tube which contains the trace gas of interest (NO_2) entrained in a flowing mixture of helium and water vapor. The NO_2(g) density was varied between 10^{13} and 10^{16} cm^{-3}. At these number densities, the N_2O_4(g) concentration is negligible (<5%). The trace gas of interest is introduced through one of three loop injectors located along the flow tube. By selecting the gas inlet port and the droplet velocity, the gas−droplet interaction time can be varied between 2 and 20 ms. The surface area of the droplets is changed in a stepwise fashion by changing the orifice driver frequency. The density of the trace gas is monitored using a quadrupole mass spectrometer.

Reaction conditions (temperature, water vapor pressure, flow rate, pressure) are carefully controlled. (See, for example, Worsnop et al.[17] and Shi et al.[19]) Overall pressure balance in the flow tube is further checked by sequentially monitoring the concentration of a reference gas, in this case krypton, which is effectively insoluble in water. Any change in krypton concentration with droplet switching determines the "zero" of the system and is subtracted from observed changes in trace gas concentration.

As shown in Worsnop et al.,[17] the measured change in trace gas signal as a function of the change in the droplet surface area yields the uptake coefficient (γ_{meas}) from which basic parameters affecting heterogeneous gas−liquid interactions can be obtained. (See next section.)

Horizontal Bubble Train Apparatus. In the horizontal bubble train flow reactor, liquid at a flow rate of 1−3 mL/s is pumped through a 0.4 cm i.d. Pyrex tube at a controlled speed of 15−35 cm s^{-1}. A low-pressure (50 Torr) gas flow, containing the trace gas of interest (NO_2) diluted in helium carrier gas, is injected into the liquid flow via 1/16 in. inconal tubing. After contact with the liquid, the NO_2(g) concentration is monitored by the quadrupole mass spectrometer. An experimental run begins with the injector positioned outside the flow tube, with the gas flowing through the injector without contacting the flowing liquid and this noncontact signal is recorded. The computer-controlled translation stage then starts to draw the injector into the flow tube filled with the flowing liquid. Well-defined bubbles, filling the diameter of the tube, are formed as the injector enters the liquid. The liquid flow carries the bubbles to the end of the flow tube, where the bubbles open and release the entrained NO_2 gas for continuous detection by the mass spectrometer. The size, speed, and frequency of the bubbles are monitored by light-emitting diodes situated 20 cm from the exit of the flow tube. The position of the injector inside the tube, as well as the speed of bubbles, defines the gas−liquid contact time, which is continuously varied in most experiments from 0.1 to 10 s. The trace gas density is recorded as a function of gas−liquid interaction time. The basic interaction parameters are extracted from such plots.

Electron impact ionization (70 eV) was used in both droplet train and bubble train studies to produce trace gas ions for mass spectrometric detection. In the ionization region, HNO_2, one of the products of NO_2 hydrolysis, readily fragments into NO_2, NO, and H, and therefore, might contribute to the NO_2 signal. However, HNO_2(aq) produced by NO_2(aq) hydrolysis is retained by the liquid because of the relatively high Henry's law coefficient of HNO_2(g) (H_{HNO_2} = 49 M atm^{-1}; 3 orders of magnitude higher than H_{NO_2}[13]). It can be shown that evaporation of HNO_2(g) from the liquid contributes less than 0.3% to the signal in the droplet studies and less than 0.1% in the bubble train studies.

The NO_2(g) used in these experiments was obtained from Aldrich Chemical Co., Inc. in the form of N_2O_4(g) (99.5%+ purity) and used without further purification. Millipore Milli-Q filtered water (resistivity >18 MΩ cm at 25 °C) was used for all of the experiments.

Modeling Gas−Liquid Interactions

In both the droplet train and the bubble train flow reactors the gas-phase species interacts with the liquid and the disappearance of that species from the gas phase is monitored. Species disappearance may be due to the entry of molecules into the bulk liquid (and possibly subsequent reactions in the bulk liquid), or to a reaction of the species at the gas−liquid interface. A key task in the development of these experimental techniques as quantitative tools has been the proper modeling of gas uptake.

In the droplet train flow reactor, gas uptake by a liquid is governed by gas-phase diffusion, mass accommodation, and often by solubility constraints as the species in the liquid approaches Henry's law saturation. In the latter process, some of the molecules that enter the liquid evaporate back into the gas phase due to the limited solubility of the trace gas. At equilibrium, the liquid is saturated and the flux of molecules into the liquid is equal to the rate of desorption of these molecules out of the liquid, resulting in zero net uptake. Chemical reactions of the solvated species in the bulk liquid or at the interface provide a sink for the species, reducing the effect of saturation. In experiments subject to these effects, the measured flux (J) into a surface is expressed in terms of a measured uptake coefficient, γ_{meas}, as

$$J = \frac{n_g \bar{c} \gamma_{meas}}{4} \quad (1)$$

where n_g is the trace gas number density and $\bar{c}$ is the average thermal speed of the trace gas molecules.

Since γ_{meas} represents a convolution of the several physical and chemical processes discussed above, the experimental challenge is to separate the contributions of these processes to the overall gas uptake. In the droplet and bubble train flow reactors the key factors affecting the rate of gas uptake are controlled, making it possible to deconvolute the uptake coefficient into its component process parameters.

General solutions to the uptake equations, which include the effect of interfacial mass accommodation, Henry's law solubility, chemical reaction in the aqueous bulk phase, and interactions at the gas−liquid interface, are not available. However, Danckwerts[20] and Sherwood and Pigford[21] provide solutions for three specific cases in the absence of gas-phase diffusion limitation: (1) uptake governed by mass accommodation and solubility, (2) uptake governed by mass accommodation, solubility, and irreversible reaction in the bulk phase liquid, and (3) uptake governed by solubility and reversible reactions. A discussion of these treatments is found in Shi et al.[19]

Modeling gas uptake in the bubble train apparatus begins with the expression for the flux, J, of gas molecules into a semi-infinite liquid in the presence of an irreversible liquid-phase chemical reaction. Since the bubble train apparatus is used to measure relatively small gas uptake ($\gamma_{meas} < 10^{-4}$), gas-phase diffusion and mass accommodation do not generally limit uptake, and their effect on uptake is considered negligible. In the absence of these two processes, for the case of irreversible reactions in the bulk liquid, Danckwerts[20] gives the following expression for the uptake flux:

$$J = n_g HRT\,[(D_l/\pi t)^{1/2}\exp(-kt) + (D_l k)^{1/2} erf(kt)^{1/2}] \quad (2)$$

Here, n_g is the gas-phase density of the trace species, R is the gas constant, D_l is the diffusion coefficient of the trace species in the liquid, k is the pseudo first-order reaction rate of the species in the liquid, T is the temperature, t is the gas−liquid interaction time, and H is the Henry's law coefficient (in M atm^{-1}).

In the limit as $k \rightarrow 0$, eq 2 yields

$$J = 2n_g HRT\,(D_l/\pi t)^{1/2} \quad (3)$$

As is evident in this case, the flux tends toward zero as the gas−liquid contact time (t) increases, and the liquid approaches saturation. In this case, if D_l is known, the Henry's law coefficient can be obtained from the uptake flux.

In the presence of an irreversible chemical reaction of the trace species in the liquid ($k \gg 0$), the solvated species is continually removed and the uptake flux approaches a steady-state value given by

$$J = n_g HRT(D_l k)^{1/2} \quad (4)$$

In this case, only the product $Hk^{1/2}$ can be obtained from uptake measurements. In the intermediate regime, where k is neither negligible nor very large, both H and the product $Hk^{1/2}$ affect the uptake.

In modeling gas uptake in the horizontal bubble train reactor, numerical techniques are used to couple the gas density in the bubble to liquid diffusion and reaction processes. The details of the model are presented in Swartz et al.[18] The model takes into account the changing size, shape, and velocity of the bubbles along their path. Model parameters were determined and the performance of the apparatus was validated by studying the uptake of five different reactive systems and eight different species with known Henry's law coefficients in the range 10^{-3} to 3.0 M atm^{-1}. For first-order reactive species, with reaction rate k, the apparatus measures $Hk^{1/2}$ values in the range 0.04−150 M atm^{-1} $s^{-1/2}$.

Modeling NO_2(g) Uptake. As was stated, NO_2(g) uptake is governed both by solubility and reactivity.

Solubility. The solvation of NO_2(g) in water as NO_2(aq) is governed by the Henry's law coefficient H_{NO_2} such that

$$[NO_2(aq)] = H_{NO_2} p_{NO_2} \quad (5)$$

where p_{NO_2} is the partial pressure of the monomer NO_2(g) in the gas phase.

At relatively high concentrations, nitrogen dioxide forms a dimer, N_2O_4, in both gas and aqueous phases. The equilibrium constants K_g and K_{aq} determine the partitioning of NO_2 and N_2O_4 in the gaseous and aqueous phases, respectively, such that

$$K_g = p_{N_2O_4}/(p_{NO_2})^2 \quad (6)$$

and

$$K_{aq} = [N_2O_4(aq)]/[NO_2(aq)]^2 \quad (7)$$

where p_{NO_2} and $p_{N_2O_4}$ are the partial pressures of NO_2(g) and N_2O_4(g), respectively.

Following the formalism of Schwartz and White,[2] we define N(IV) as the nitrogen species in the oxidation state IV, such that the concentration $[N(IV)_{aq}]$ in aqueous solution, and the partial pressure of $N(IV)_g$ in the gas phase, $p_{N(IV)}$, are given as follows:

$$[N(IV)_{aq}] = [NO_2(aq)] + 2[N_2O_4(aq)] = [NO_2(aq)] + 2K_{aq}[NO_2(aq)]^2 \quad (8)$$

and

$$p_{N(IV)} = p_{NO_2} + 2p_{N_2O_4} = p_{NO_2} + 2K_g(p_{NO_2})^2 \quad (9)$$

Because NO_2(aq) and N_2O_4(aq) rapidly reach equilibrium, the solubility of $N(IV)_g$ is represented by an effective Henry's law coefficient

$$H_{eff} = \frac{[N(IV)_{aq}]}{p_{N(IV)}} = \frac{H_{NO_2}(1 + 2K_{aq}H_{NO_2}p_{NO_2})}{(1 + 2K_g p_{NO_2})} \quad (10a)$$

Under our experimental conditions where p_{NO_2} is low, $2K_g p_{NO_2} \ll 1$, and H_{eff} is approximated by

$$H_{eff} = H_{NO_2}(1 + 2K_{aq}H_{NO_2}p_{NO_2}) \quad (10b)$$

which is now the effective Henry's law coefficient for NO_2(g).

It is evident from eq 10b that solubility experiments performed at low NO_2(g) concentration, such that $2K_{aq}H_{NO_2}p_{NO_2} \ll 1$, can yield values for H_{NO_2}.

Reactivity. When NO_2(g) enters water it forms the acids HNO_2(aq) and HNO_3(aq) either via the reaction R1

$$2NO_2(aq) + H_2O(l) \xrightarrow{k'} HNO_2(aq) + HNO_3(aq) \quad (R1)$$

or via reaction R2

$$2NO_2(aq) + H_2O(l) \underset{k_{bac}}{\overset{k_{for}}{\rightleftharpoons}} N_2O_4(aq) + H_2O(l) \xrightarrow{k''} HNO_2(aq) + HNO_3(aq) \quad (R2)$$

Both processes R1 and R2 are considered irreversible because the reverse rates are slow compared to the gas−liquid interaction times in the droplet and bubble train apparatuses. As shown in the Appendix, the disappearance of NO_2(aq) is second-order in NO_2(aq) concentration for both pathways R1 and R2. Therefore, NO_2(aq) disappearance can be described by

$$-\frac{d[NO_2(aq)]}{dt} = 2k_2[NO_2(aq)]^2 \quad (11a)$$

where the NO_2(aq)−NO_2(aq) hydrolysis rate coefficient (k_2) is equal to the summation of the rates for the two reaction pathways.

$$k_2 = k' + k''K_{aq} \quad (11b)$$

The reactive disappearance of $N(IV)_{aq}$ concentration, however, is of mixed order in $N(IV)_{aq}$ concentration because the reaction is first-order in N_2O_4(aq). (For details see Schwartz and White.[2])

By conservation of mass, the gas flux into the liquid is equal to the removal flux of liquid-phase species away from the interface. Because NO_2(g) rapidly partitions into NO_2(aq) and N_2O_4(aq) upon solvation, the NO_2(g) uptake flux in our experiments is equal to this $N(IV)_{aq}$ flux leaving the interface.

The analytical solution of Danckwerts,[20] eq 2, is valid for first-order kinetics in the liquid phase. Because the kinetics of $N(IV)_{aq}$ are of mixed order, the Danckwerts expression is not directly applicable to our system. This mixed-order kinetics is taken into account using the results of Brian.[22] Brian[22] numerically calculated the gas uptake rate for the case where the aqueous-phase reaction can be represented by a rate equation of order n (n not necessarily an integer) and rate coefficient k_F as

$$\frac{d[N(IV)_{aq}]}{dt} = -k_F[N(IV)_{aq}]^n \quad (12)$$

The results of Brian[22] show that such a mixed-order uptake flux can be approximated (to within 3%) by replacing k in eq 2 with

$$k = \frac{2}{n+1}k_F[N(IV)_{aq}]_0^{(n-1)} \quad (13)$$

where $[N(IV)_{aq}]_0$ is the surface $N(IV)_{aq}$ concentration. In our experiment, the surface is close to equilibrium with the gas phase, yielding $[N(IV)_{aq}]_0 = H_{eff}p_{NO_2}$.

We show in the Appendix that k_F can be expressed as

$$k_F = \frac{2k_2[NO_2(aq)]^2}{[N(IV)_{aq}]^n} = \frac{2k_2[NO_2(aq)]^2}{([NO_2(aq)] + 2[N_2O_4(aq)])^n} \quad (14)$$

An analytical expression for n is not available. We approximate n by the following expression:

$$n = 2 - \frac{2[N_2O_4(aq)]}{[N(IV)_{aq}]} = 2 - \frac{2[N_2O_4(aq)]}{[NO_2(aq)] + 2[N_2O_4(aq)]} \quad (15)$$

This simple formulation has the required behavior that n varies from 2 when NO_2(aq) is the dominant reacting species to 1 when N_2O_4(aq) dominates. We have tested several other expressions for n that provide a reasonable variation between 1 and 2 as a function of NO_2(aq) density. The model is relatively insensitive to the form of n. All the functions tried yield values of $H_{NO_2}k_2^{1/2}$ within 5% of each other.

As is evident in eq 2, the NO_2(g) flux (uptake) into the liquid is a function of H_{eff} and the rate constant k, now defined in eq 13. Therefore, measurement of the gas uptake flux yields k_F which in turn, via eq 14, yields k_2. Since both parameters are functions of NO_2(g) concentration, the NO_2(g) uptake has a nonlinear dependence on the NO_2(g) concentration. (See eq 10a and 13.) Since both H_{eff} and k decrease with NO_2(g) concentration, the normalized NO_2(g) uptake flux decreases with NO_2(g) concentration. Further, at sufficiently low NO_2(g) concentrations, the reactive component of the uptake is negligible, and $H_{eff} \approx H_{NO_2}$. In this region, the uptake is determined entirely by the H_{NO_2} solubility and the normalized uptake flux is independent of NO_2(g) concentration. In this regime, the gas uptake measurements yield the physical Henry's law solubility.

At this point, we note an important aspect of the numerical model used in data analysis. The bubble train reactor was originally calibrated for pseudo-first-order reactions.[18] It was found that in the range of lower reactive uptake, a parameter (designated f_D) had to be introduced to account for an enhanced observed uptake. The parameter f_D varied between 3.4 at low $Hk^{1/2}$ to 1 at high $Hk^{1/2}$. This observed enhancement was attributed to postulated small-scale eddy currents within the liquid which preferentially enhance uptake by removing solvated molecules from the interface and returning the molecules at a lower concentration because some of the molecules have reacted away in transit. (For a more detailed discussion, see Swartz et al.[18]) For second-order reactions in the aqueous phase, the effect of these eddy currents on uptake is expected to be diminished because of the reduced effect of the reactions in transit. As the solvated species is removed from the interface by the eddy currents, they are brought into areas of lower NO_2(aq) concentration, and hence the effective reaction rate is also lower. When these molecules are subsequently returned to the surface by the eddy currents, their concentration is less depleted, and the resultant uptake enhancement is then less than for the corresponding first-order reaction. The best fit to the NO_2(g) uptake data is obtained with $f_D = 1$.

Results and Discussion

Uptake of NO_2(g) in the Droplet Train Apparatus. In our droplet experiments, the uptake coefficient (γ_{meas}) for NO_2(g) was measured at $T = 273$ K with gas-liquid interaction times ranging from 1.6 to 17.2 ms, and with the trace gas number density ranging from 10^{13} to 10^{16} cm^{-3}. The uptake of NO_2(g) was below the sensitivity limit of the apparatus at all gas densities and interaction times studied, which sets the limit on the uptake coefficient of $\gamma_{meas} < 5 \times 10^{-4}$ at 273 K. The Mertes and Wahner[9] studies yielded density-dependent uptake coefficients of $\gamma_{meas} = (2.4 \pm 1.4) \times 10^{-4}$ at NO_2(g) density of 9×10^{14} cm^{-3} and $\gamma_{meas} = (1.2 \pm 0.4) \times 10^{-3}$ at NO_2(g) density 8×10^{15} cm^{-3} at 298 K. Ponche et al.[8] measured uptake coefficients of $\gamma_{meas} = (1.5 \pm 0.6) \times 10^{-3}$ at NO_2(g) density of 9×10^{14} cm^{-3} at 290 K. The latter two values are an order of magnitude higher than our upper limit. We do not have a clear explanation for this difference. However, we note that neither Ponche et al.[8] nor Mertes and Wahner[9] used a reference gas to account for the sweep-out of the gas by the moving liquid. While this effect may not be of significance in the jet experiment of Mertes and Wahner,[9] in the droplet experiment, the sweep-out can yield an artifact of $\gamma_{meas} = 10^{-3}$.

The NO_2(g) uptake coefficient calculated via eqs 1 and 2 solely on the basis of bulk-phase solubility and NO_2(aq) hydrolysis is, at most, $\gamma_{meas} = 10^{-5}$. (This maximum value is obtained at the shortest gas−liquid interaction time and the

TABLE 1: Values for NO_2(g) of the Henry's Law Coefficient, H_{NO_2}, the Second-Order Rate Coefficient of NO_2(aq)−NO_2(aq) Hydrolysis, k_2, and the Product $H_{NO_2}k_2^{1/2}$ (primary measurements are indicated in bold)

reference	$Hk_2^{1/2}$ ($M^{1/2}$ atm^{-1} $s^{-1/2}$)	H × 10^2 (M atm^{-1})	k_2 × 10^{-7} (M^{-1} s^{-1})
this work	**71 ± 10**[a]	**1.4 ± 0.2**	2.7 ± 0.7
gas uptake measurements			
Komiyama and Inoue[30]		**2.0 ± 0.3**[b]	
Lee and Schwartz[10]	**70 ± 9**[c]		2.5 ± 0.6
Park and Lee[13]	**92 ± 20**[c]		4.3 ± 1.9
Cape et al.[11]	**106 ± 20**[d]		5.7 ± 2.2
aqueous phase concentration decay measurements			
Moll[14]			**2.6**[e]
Grätzel et al.[15]			**6.5 ± 0.7**[a]
Treinin and Haydon[16]			**4.7 ± 1.0**[f]
recommended values		1.4 ± 0.2	3.0 ± 0.9

[a] At 293 K, with $D_1 = 1.23 \times 10^{-5}$ cm^2 s^{-1}. [b] Adjusted from 288 K to 293 K using heat of solution of O_3 (4.6 kcal/mol, Kosak-Channing and Helz[25]) and $D_1 = 1.1 \times 10^{-5}$ cm^2 s^{-1} at 288 K. Original paper did not cite a value for measurement uncertainty. A ±15% uncertainty is assumed (see text). [c] At 295 K. [d] Adjusted from 283 K to 293 K (see text). [e] At 293 K. Revised according to Schwartz and White.[2] Literature review did not cite a value for measurement uncertainty. [f] At 298 K.

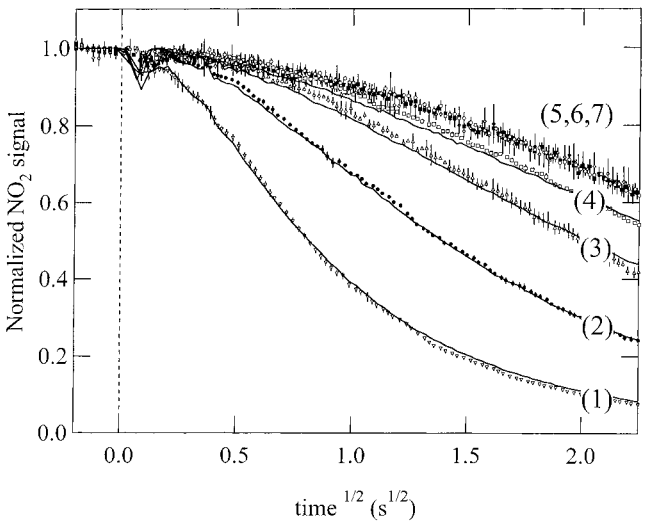

Figure 1. Uptake of NO_2(g) by water at 293 K as a function of the square root of gas−liquid interaction time ($t^{1/2}$). Initial NO_2(g) number density: (1) 8.6 × 10^{16} cm^{-3}; (2) 2.3 × 10^{16} cm^{-3}; (3) 9.5 × 10^{15} cm^{-3}; (4) 4.1 × 10^{15} cm^{-3}; (5) 1.5 × 10^{15} cm^{-3}; (6) 6.5 × 10^{14} cm^{-3}; (7) 2.3 × 10^{14} cm^{-3}.

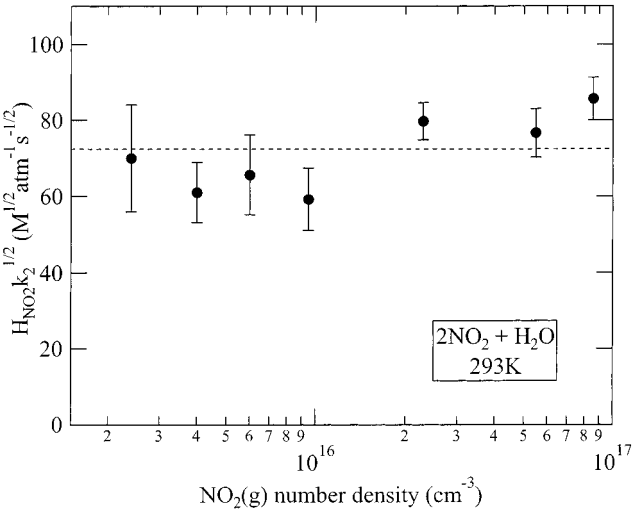

Figure 2. Best-fit values of $H_{NO_2}k_2^{1/2}$ as a function of initial NO_2(g) number density. The average value $H_{NO_2}k_2^{1/2} = 71$ $M^{1/2}$ atm^{-1} $s^{-1/2}$ is shown as a dotted line.

highest k_2 and H_{NO_2} published in the literature, see Table 1.) The upper limit of $\gamma_{meas} < 5 \times 10^{-4}$ obtained with our droplet apparatus is consistent with NO_2(g) uptake governed by bulk-phase processes. The results do not provide evidence for a surface reaction of the magnitude suggested by Mertes and Wahner.[9]

NO_2 Uptake in the Horizontal Bubble Train Reactor. The uptake of NO_2(g) in the bubble train flow reactor was studied at NO_2(g) densities (at $t = 0$) ranging from 8 × 10^{13} to 8 × 10^{16} cm^{-3} and at two temperatures, 293 and 276 K. In Figure 1 we show the normalized density of the gas-phase species as a function of the square root of the interaction time. This set of data was obtained at 293 K. The NO_2(g) densities are indicated in the figure caption. For clarity of presentation, data are not displayed for all NO_2(g) density studies. Model fits to the data sets 1 to 4 are shown as solid lines. (See further discussion.)

As expected, because of the NO_2(aq) reactions, the uptake is largest at the highest NO_2(g) densities. The uptake decreases as the NO_2(g) density is lowered and becomes independent of gas density for NO_2(g) densities less than 1.5 × 10^{15} cm^{-3}. In this regime, uptake is determined by solubility, with $H_{eff} = H_{NO_2}$ (see eq 10b). The numerical model fit to the data yields H_{NO_2} = (1.4 ± 0.2) × 10^{-2} M atm^{-1} at 293 K. The liquid-phase diffusion coefficient for NO_2(aq) used in the model calculation is 1.23 × 10^{-5} cm^2 s^{-1} calculated using the cubic cell model.[23]

Our results yield an upper limit on the magnitude of the equilibrium coefficient, K_{aq} as follows. In the region of measurements, a difference in the uptake due to about an 8% change in Henry's law coefficient can be distinguished.[17] In the NO_2 density region between 2.3 × 10^{14} cm^{-3} and 1.5 × 10^{15} cm^{-3} the uptake data are, within the accuracy of our measurement, independent of NO_2 density. (See Figure 1.) This implies that up to a NO_2 density of about 1.5 × 10^{15} cm^{-3}, the term $2K_{aq}H_{NO_2}p_{NO_2}$ in eq 10b is negligible compared to 1. In turn, this puts a constraint on the equilibrium constant K_{aq} to be less than 6 × 10^4 M^{-1}, in agreement with the measurement of Grätzel et al.,[15] $K_{aq} = (6.5 \pm 0.3) \times 10^4$ M^{-1} at 293 K.

To extract values for the rate coefficient k_2, the uptake data traces 1 to 4 in Figure 1 were fit by the model with k_2 as the variable, using the above-stated values, $H_{NO_2} = 1.4 \times 10^{-2}$ M atm^{-1} and $K_{aq} = 6.5 \times 10^4$ M^{-1}. Since most of the previous gas uptake measurements yielded the product $H_{NO_2}k_2^{1/2}$, for purposes of comparison, we present our results in the same form. In Figure 2, $H_{NO_2}k_2^{1/2}$ is presented as a function of the initial NO_2(g) density. The error bars represent an uncertainty of one standard deviation of k_2 to the model fit. The dashed line in the figure is the average of these and yields $H_{NO_2}k_2^{1/2} = (71 \pm 10)$ $M^{1/2}$ atm^{-1} $s^{-1/2}$ at 293 K. The uncertainty in the quoted

$H_{NO_2}k_2^{1/2}$ value is the statistical uncertainty representing one standard deviation from the average.

The uptake of NO_2(g) at 276 K was also measured as a function of gas density. The studies at this temperature did not yield the clear separation between reactive- and solubility-governed uptake that was obtained at 293 K principally because at this temperature, K_{aq} is significantly higher than at 293 K. Therefore, even at the limit of our NO_2(g) detection sensitivity, H_{eff} is larger than H_{NO_2}, and the uptake does not converge even at the lowest NO_2(g) density accessible in this experiment. However, uptake at the lowest NO_2(g) density (2.8×10^{14} cm^{-3}) does yield an upper limit to $H_{NO_2} < 2.3 \times 10^{-2}$ M atm^{-1} at 276 K. Schwartz and White,[24] suggested on the basis of the similarity in molecular structure between NO_2(g) and O_3(g), that the heat of solution of O_3(g) may be used to estimate the temperature dependence of H_{NO_2}. Using this value (−4.6 kcal mol^{-1}, Kosak-Channing and Heltz[25]), the predicted H_{NO_2} at 276 K is 2.3×10^{-2} M atm^{-1} in agreement with our upper limit. We suggest that in the absence of clear experimental results, the value of $H_{NO_2} = 2.3 \times 10^{-2}$ M atm^{-1} at 276 K be used.

Further, Schwartz and White[2] suggest a temperature dependence for $H_{NO_2}k_2^{1/2}$ based on the temperature dependence of nitrous acid decomposition measured by Abel et al.[26] Using this temperature dependence, given by exp (3.9 kcal mol^{-1}/RT), we extrapolate our measurement at 293 K to obtain $H_{NO_2}k_2^{1/2} = (107 \pm 15)$ M$^{1/2}$ atm^{-1} s$^{-1/2}$ at 276 K. With $H_{NO_2} = 2.3 \times 10^{-2}$ M atm^{-1}, this yields an estimated value for $k_2 = (2.2 \pm 0.6) \times 10^7$ M^{-1} s^{-1} at 276 K. Using the above stated values of H_{NO_2} and $H_{NO_2}k_2^{1/2}$, we fit our uptake data to obtain $K_{aq} = (3.5 \pm 1.5) \times 10^5$ M^{-1}.

The results of the bubble train uptake experiments provide further confirmation that a reactive NO_2 surface complex is not involved in the uptake process. The Mertes and Wahner[9] value of $\gamma_{meas} = (1.2 \pm 0.4) \times 10^{-3}$ at NO_2(g) density 8×10^{15} cm^{-3} is attributed in their work to the surface complex and its reaction. While in the droplet train experiment, this value of γ_{meas} is near the detection limit of the apparatus, in the bubble train experiment, an uptake coefficient of this magnitude would manifest as an almost instantaneous depletion (10 ms) of the species from the gas phase. This is clearly not the case as is evident in Figure 1. Even after 4 s, only 50% of the NO_2(g) is depleted.

Another type of surface reaction has been reported by several investigators who measured the disappearance of NO_2(g) in the presence of various humid surfaces.[27−29] These reactions are first-order in NO_2(g) and are relatively slow. Using the formalism of Lammel and Cape,[1] it can be shown that the measured surface reaction rates are 5 orders of magnitude lower than those suggested in the Mertes and Wahner[9] study, and contribute less than 1% to the uptake observed in the bubble train experiments.

Comparison with Previous Results. Literature values for the Henry's law coefficient, H_{NO_2}, the rate coefficient, k_2, and the product, $H_{NO_2}k_2^{1/2}$, together with our values for these parameters are shown in Table 1. The primary measured parameters are in bold print for each study. Previous measurements of k_2 fall into two categories: NO_2(g) uptake measurements from vertically rising bubbles, and concentration decay measurements of NO_2(aq) and N_2O_4(aq) in aqueous phase. The literature also contains several high-concentration NO_2(g) uptake studies which are more difficult to interpret and are not included in Table 1. (For a review of these studies, see Schwartz and White[2]).

As shown in the footnotes to Table 1, most of the measurements were conducted in the temperature range 293 to 298 K, except for those of Komiyama and Inoue[30] and Cape et al.[11] These two studies were done at 288 and 283 K, respectively. For purposes of comparison, the results from these experiments were extrapolated to 293 K using the temperature dependences for H_{NO_2} and $H_{NO_2}k_2^{1/2}$ discussed earlier. The value of H_{NO_2} from the Komiyama and Inoue[30] study was further adjusted to take into account the difference between their estimate of the liquid-phase diffusion coefficient ($D_l = 1.0 \times 10^{-5}$ cm^2 s^{-1} at 288 K), and the more accurate value of Houghton[23] ($D_l = 1.1 \times 10^{-5}$ cm^2 s^{-1} at 288 K).

In our work, both $H_{NO_2}k_2^{1/2}$ and at low densities, the independent value of H_{NO_2} were measured. Of the other studies listed in Table 1, only that of Komiyama and Inoue[30] yielded an independent value of H_{NO_2}. In the other studies, only the product $H_{NO_2}k_2^{1/2}$ was directly measured; H_{NO_2} values quoted in these studies were not measured directly and are not listed in the table. While values for experimental uncertainty were not presented in the original Komiyama and Inoue paper,[30] a ±15% uncertainty is typical of such studies. As is evident, the two independent measurements of H_{NO_2} are in agreement within experimental uncertainty. In the Komiyama and Inoue experiments, the apparatus was calibrated at only one value of H, that of CO_2. The bubble train apparatus has been calibrated for a wide range of Henry's law coefficients. Based on these calibrations,[18] our recommended value for H_{NO_2} at 293 K is $(1.4 \pm 0.2) \times 10^{-2}$ M atm^{-1}.

As stated above, in gas uptake studies where the effect of liquid-phase reactions is significant, solubility and reactivity are coupled such that only the product $H_{NO_2}k_2^{1/2}$ is measured. The product $H_{NO_2}k_2^{1/2}$ measured in these experiments are shown in Table 1. In the original literature, uncertainties in the product are not listed. The uncertainty values in Table 1 were obtained from the quoted uncertainties in the extrapolated values of H_{NO_2} and k_2. The corresponding value of k_2 listed in the last column of Table 1 were calculated from the product $H_{NO_2}k_2^{1/2}$ using our recommended value of $H_{NO_2} = 1.4 \times 10^{-2}$ M atm^{-1}. With the exception of the Cape et al. study,[11] all the measured values of $H_{NO_2}k_2^{1/2}$ are within experimental uncertainty of each other.

The three k_2 values listed in the last grouping of Table 1, were obtained from concentration decay measurements. Although this technique appears to be the most straightforward, examination of the experimental conditions of Grätzel et al.[15] and Treinin and Haydon[16] reveals complications. Since the NO_2(aq) decay is second-order, extrapolation of k_2 from the decay results requires an accurate knowledge of NO_2(aq) density. These densities, which were measured by optical absorption, rely on the knowledge of the extinction coefficient in water. The original extinction coefficient measurements assumed that the following reaction proceeds rapidly and completely:

$$OH(aq) + NO_2^-(aq) \rightarrow OH^-(aq) + NO_2(aq)$$

Due to the high reactivity of the OH radical, any impurities in the solution would cause a depletion of OH and an overestimation of the NO_2(aq) extinction coefficient. As a result, NO_2(aq) concentration would be underestimated, and k_2 overestimated. The magnitude of this effect cannot be determined at this point.

The experiments of Moll[14] were done differently. Here, liquid N_2O_4 was injected into a turbulent water flow, and the extent of the N_2O_4(aq)−water reaction (see R2) was monitored by the temperature profile downstream. This is a first-order reaction, yielding k' in reaction R2. The rate coefficient k_2 is then obtained via $k_2 = K_{aq}k'$. In this experiment, a measurement of NO_2(aq)

concentration is not required. We consider this result the most accurate of the decay studies.

In the final row of Table 1, we list our recommended value for k_2 (293 K) which is a simple average of the k_2 values excluding the values of Cape et al.,[11] Grätzel et al.,[15] and Treinin and Haydon.[16] This value is $k_2 = (3.0 \pm 0.9) \times 10^7$ M^{-1} s^{-1}.

Summary

The results of NO_2(g) uptake studies using a bubble train flow reactor, and an analysis of literature values yield the following values for the Henry's law coefficient, H_{NO_2}, and the second-order NO_2(aq)−NO_2(aq) hydrolysis reaction rate coefficient, k_2. At 293 K $H_{NO_2} = (1.4 \pm 0.2) \times 10^{-2}$ M atm^{-1} and $k_2 = (3.0 \pm 0.9) \times 10^7$ M^{-1} s^{-1}. At 276 K, $H_{NO_2} = 2.3$ (+0.3−0.9) $\times 10^{-2}$ M atm^{-1} and $k_2 = (2.2 \pm 0.6) \times 10^7$ M^{-1} s^{-1}. Evidence for an NO_2 heterogeneous reaction at the surface of pure water, suggested in the literature,[7−9] was not observed.

Acknowledgment. Funding for this work was provided by the National Science Foundation Grants No. ATM-96-32599, the U.S. Environmental Protection Agency Grant No. R-821256-01-0, and Department of Energy Grants No. DE-FG02-91ER61208 and DE-FG 02-98ER62581.

Appendix

We derive here an expression for k_F as presented in eq 14. We proceed as follows. (I) As stated in the text, the rate equation governing the disappearance of $N(IV)_{aq}$ and therefore also for NO_2(g) is of mixed order. However, as will be shown, the disappearance of NO_2(aq) is purely second-order. (II) As a consequence of I, $N(IV)_{aq}$ disappearance is also second-order in NO_2(aq). (III) Derivation of I and II leads to eq 14.

(I) As shown in the text, NO_2(aq)−NO_2(aq) hydrolysis occurs via channels R1 and R2. The rate of the reaction is the sum of these two channels:

$$-\frac{d[NO_2(aq)]}{dt} = 2k'[NO_2(aq)]^2 + 2k''[N_2O_4(aq)] \quad (A1)$$

Since the NO_2(aq)−N_2O_4(aq) equilibrium is established more rapidly than the overall hydrolysis reaction,[2] then

$$[N_2O_4(aq)] = K_{aq}[NO_2(aq)]^2$$

thus

$$-\frac{d[NO_2(aq)]}{dt} = 2k'[NO_2(aq)]^2 + 2k''_{aq}[NO_2(aq)]^2$$
$$= 2(k' + k''K_{aq})[NO_2(aq)]^2 \quad (A2)$$

The disappearance of NO_2(aq) is second-order in NO_2(aq) concentration for either mechanism. Since the NO_2(aq)−NO_2(aq) hydrolysis rate coefficient is defined from the equation

$$-\frac{d[NO_2(aq)]}{dt} = 2k_2[NO_2(aq)]^2$$

we obtain by inspection,

$$k_2 = k' + K_{aq}k'' \quad (A3)$$

(II) We have defined $[N(IV)(aq)] = [NO_2(aq)] + 2[N_2O_4(aq)]$, thus,

$$-\frac{d[N(IV)_{aq}]}{dt} = -\frac{d[NO_2(aq)]}{dt} - 2\frac{d[N_2O_4(aq)]}{dt}$$

where,

$$-\frac{d[NO_2(aq)]}{dt} = 2k'[NO_2(aq)]^2 + 2k_{for}[NO_2(aq)]^2 - 2k_{bac}[N_2O_4(aq)]$$

and

$$-\frac{d[N_2O_4(aq)]}{dt} = k''[N_2O_4(aq)] + k_{for}[NO_2(aq)]^2 - k_{bac}[N_2O_4(aq)]$$

Therefore,

$$-\frac{d[N(IV)_{aq}]}{dt} = 2k'[NO_2(aq)]^2 + 2k''[N_2O_4(aq)]$$
$$= 2k'[NO_2(aq)]^2 + 2k''K_{aq}[NO_2(aq)]^2$$
$$= 2(k' + k''K_{aq})[NO_2(aq)]^2$$

Then, according to eq A3,

$$-\frac{d[N(IV)_{aq}]}{dt} = 2k_2[NO_2(aq)]^2 \quad (A4)$$

(III) As stated in the text, the expression of Brian[22] used here is

$$\frac{d[N(IV)_{aq}]}{dt} = -k_F[N(IV)_{aq}]^n \quad (A5)$$

Rearranging this expression yields

$$k_F = \frac{1}{[N(IV)_{aq}]^n}\left\{-\frac{d[N(IV)_{aq}]}{dt}\right\}$$

Substituting A3 for the derivative and eq 8 for the $N(IV)_{aq}$ yields eq 14:

$$k_F = \frac{2k_2[NO_2(aq)]^2}{[N(IV)_{aq}]^n} = \frac{2k_2[NO_2(aq)]^2}{([NO_2(aq)] + 2[N_2O_4(aq)])^n}$$

References and Notes

(1) Lammel, G.; Cape, J. N. *Chem. Soc. Rev.* **1996**, 361−369.
(2) Schwartz, S. E.; White, W. H. Kinetics of reactive dissolution of nitrogen oxides into aqueous solution. In *Advances in Environmental Science and Technology*; Schwartz, S. E., Ed.; Wiley: New York, 1983; Vol. 12, pp 1−116.
(3) Hauglustaine, D. A.; Ridley, B. A.; Solomon, S.; Hess, P. G.; Madronich, S.; *Geophys. Res. Lett.* **1996**, *23*, 2609−2612.
(4) Amman, M.; Kalberer, M.; Jost, D. T.; Tobler, L.; Rössler, E.; Piguet, D.; Gäggeler, H. W.; Baltensperger, U. *Nature* **1998**, *395*, 157−160.
(5) Kleffmann J.; Becker K. H.; Wiesen P. *Atmos. Environ.* **1998**, *32*, 2721−2729.
(6) Aumont, B.; Madronich, S.; Amman, M.; Kalberer, M.; Baltensperger, U.; Hauglustaine, D.; Brocheton, F. *J. Geophys. Res.* **1999**, *104*, 1729−1736.
(7) Finlayson-Pitts, B. J.; Pitts, J. N., Jr. *Chemistry of the Upper and Lower Atmosphere*; Academic Press: San Diego, 2000; pp 268−271.
(8) Ponche, J. L.; George, Ch.; Mirabel, Ph. *J. Atmos. Chem.* **1993**, *16*, 1−21.
(9) Mertes, S.; Wahner, A. *J. Phys. Chem.* **1995**, *99*, 14000−14006.
(10) Lee, Y.-N.; Schwartz, S. E. *J. Phys. Chem.* **1981**, *85*, 840−848.

(11) Cape, J. N.; Storeton-West, R. L.; Devine, S. F.; Beatty, R. N.; Murdoch, A. *Atmos. Environ.* **1993**, *27A*, 2613−2621.
(12) Bambauer, A.; Brantner, B.; Paige, M.; Novakov, T. *Atmos. Environ.* **1994**, *28*, 3225−3232.
(13) Park, J.-Y.; Lee, Y.-N. *J. Phys. Chem.* **1988**, *92*, 6294−6302.
(14) Moll, A. J. The rate of hydrolysis of nitrogen tetroxide. Ph.D. Thesis, University of Washington, 1966.
(15) Grätzel, M.; Henglein, A.; Little, J.; Beck, G. *Ber. Bunsen-Ges.* **1969**, *73*, 646−653.
(16) Treinin, A.; Haydon, E. *J. Am. Chem. Soc.* **1970**, *92*, 5821−5828.
(17) Worsnop, D. R.; Zahniser, M. S.; Kolb, C. E.; Gardner, J. A.; Watson, L. R.; Van Doren, J. M.; Jayne, J. T.; Davidovits, P. *J. Phys. Chem.* **1989**, *93*, 1159−1172.
(18) Swartz, E.; Boniface, J.; Tchertkov, I.; Rattigan, O.; Robinson, D. V.; Davidovits, P.; Worsnop, D. R.; Jayne, J. T.; Kolb, C. E. *Environ. Sci. Technol.* **1997**, *31*, 2634−2641.
(19) Shi, Q.; Davidovits, P.; Jayne, J. T.; Worsnop, D. R.; Kolb, C. E. *J. Phys. Chem. A* **1999**, *103*, 8812−8823.
(20) Danckwerts, P. V. *Gas−Liquid Reactions*, McGraw-Hill: New York, 1970; Chapter 3.
(21) Sherwood, T. K.; Pigford, R. L. *Absorption and Extraction*, 2nd ed.; McGraw-Hill: New York, 1952; p 329.
(22) Brian, P. L. T. *Am. Inst. Chem. Eng. J.* **1964**, *10*, 5−10.
(23) Houghton, G. *J. Chem. Phys.* **1964**, *40*, 1628.
(24) Schwartz, S. E.; White, W. H. Solubility equilibria of the nitrogen oxides and oxyacids in dilute aqueous solution. In *Advances in Environmental Science and Engineering*; Pfafflin, J. R., Ziegler, E. N., Eds.; Gordon and Breach: New York, 1981; Vol. 4, pp 1−45.
(25) Kosak-Channing, L. F.; Helz, G. R. *Environ. Sci. Technol.* **1983**, *17*, 145−149.
(26) Abel, E.; Schmid, H.; Romer, E. Kinetics of nitrous acid. VII. Rate and temperature. *Z. Phys. Chem.* **1930**, *148*, 337−349.
(27) Sakamaki, F.; Hatakeyama, S.; Akimoto, H. *Int. J. Chem. Kinet.* **1983**, *15*, 1013.
(28) Pitts, J. N.; Sanhueza, E.; Atkinson, R.; Carter, W. P. L.; Winer, A. M.; Harris, G. W.; Plum, Ch. N. *Int. J. Chem. Kinet.* **1984**, *16*, 919.
(29) Svensson, R.; Ljungström, E.; Lindqvist, O. *Atmos. Environ.* **1987**, *21*, 1529−1539.
(30) Komiyama, H.; Inoue, M. *Chem. Eng. Sci.* **1980**, *35*, 154−161.